

## Identification of Alcohol Adsorption Sites on $\gamma$ -Alumina

E. C. DECANIO,<sup>\*,†,1</sup> V. P. NERO,<sup>\*</sup> AND J. W. BRUNO<sup>†</sup>

<sup>\*</sup>Texaco Research and Development Department, P.O. Box 509, Beacon, New York 12508 and

<sup>†</sup>Wesleyan University, Middletown, Connecticut 06459

Received October 22, 1991; revised January 14, 1992

A novel temperature-programmed desorption technique in which the probe of a mass spectrometer is used as the reactor has been developed. FT-IR and this new technique have been used to study the adsorption and dehydration reactions of a series of aliphatic alcohols on  $\gamma$ -alumina. It was found that the facility with which the various alkoxides undergo elimination processes is dependent on the size of the alkyl groups and the degree of branching. Reactions involving [<sup>18</sup>O]ethanol and [<sup>18</sup>O]methanol produce two isotomeric ether products ( $R^{18}OR$  and  $R^{16}OR$ ), which shows that bound alkoxides are formed by two routes; (a) dissociative adsorption on Lewis acid sites and (b) nucleophilic attack by a surface oxide on an alcohol that is probably activated toward C–O cleavage. Poisoning experiments using 2,6-dimethylpyridine confirm that the ether isotopomers are formed from different alkoxide species. Time studies indicate that there is no scrambling of the <sup>16</sup>O and <sup>18</sup>O alkoxides between the different types of surface sites. © 1992 Academic Press, Inc.

### INTRODUCTION

The acid–base properties of metal oxide supports can have a significant effect on the product selectivities exhibited by heterogeneous catalysts (1–5). One of the most common supports in heterogeneous catalysis is  $\gamma$ -alumina, and there has been much work carried out in order to understand the structure of the alumina surface and nature of the acid–base sites (6, 7).

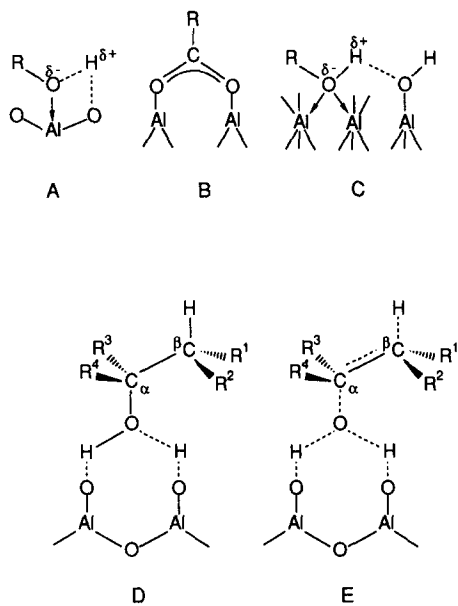
The acid–base properties of metal oxides are often investigated by studying the product selectivities of the reactions of alcohols (8–11). This has led to several infrared and gravimetric studies of the adsorbed alcohols (12–17). Based on these it was concluded that there are three types of species produced when short chain alcohols are chemisorbed onto calcined  $\gamma$ -alumina. One such species (**A**) (Structure 1) is produced when the alcohol is chemisorbed onto a coordinatively unsaturated aluminum ion (Lewis acid site). Lateral H-bonding interactions between the alcohol OH group and an adja-

cent group (such as O<sup>−</sup>) contribute to the alcohol OH bond breaking; this species may be considered to be a precursor state in dissociative chemisorption (15, 16).

The second chemisorption species has a carboxylate structure (**B**) and is formed at higher temperatures (12, 13). The third moiety consists of an alcohol adsorbed onto an acid–base pair site, which has an exposed pair of coordinatively unsaturated Al<sup>3+</sup> ions in an anion vacancy in the vicinity of a type Ia or Ib hydroxyl group (type Ia and Ib, etc., are the hydroxyl groups in the model developed by Knözinger to describe the hydroxyl structure of the alumina surface (6)). In the species depicted in **C** the alcohol is coordinated to a type IIa site in a bridging manner, and the neighboring most basic type Ia group then offers a lone pair of electrons for interaction with the alcohol proton.

By comparing the C–H stretching frequency changes as various alcohols were adsorbed, Lavally *et al.* (17) concluded that species **A** is formed irreversibly while species **C** is, in part, formed reversibly. This is in agreement with Knözinger and Stubner (16), who also suggested that species **C**

<sup>1</sup> To whom correspondence should be addressed.



STRUCTURE I

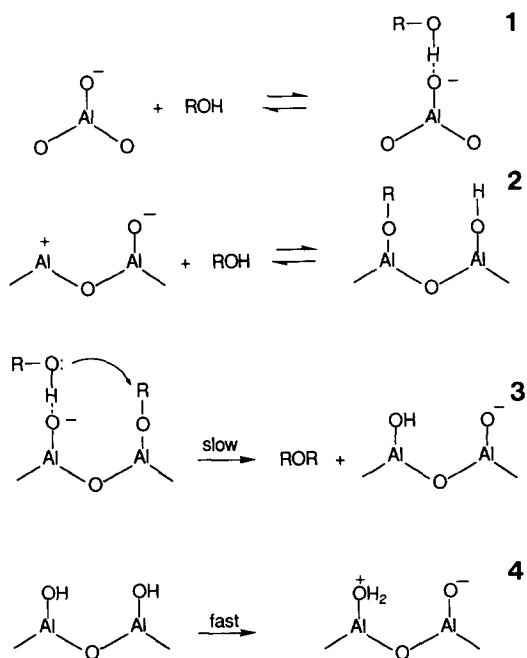
would be formed as long as an alcohol is adsorbed on a suitable acid–base site. The nature of the acid–base site would therefore determine whether the chemisorption is reversible or not.

Concurrent with these IR studies, there were a considerable number of studies aimed at understanding the kinetic and mechanistic aspects of the dehydration reactions leading to ether and alkene formation (7, 18–27). The early catalytic studies showed that the alumina–alcohol interaction was not simple (20). Rate vs partial pressure studies and poisoning experiments by Jain and Pillai (21) and work carried out by de Mourges *et al.* (22) indicated that ether and olefin formation requires different types of sites. The results of Jain and Pillai (21) showed that ether formation required adjacent acid–base sites while olefin formation required stronger acid sites only. This work also showed that ether formation occurred via a bimolecular reaction between an alkoxide species and a strongly adsorbed alcohol. Similar mechanistic models were developed by Knözinger *et al.* (23) and

Padmanabhan and Eastburn (24). The basic scheme is shown in Scheme 1. Presumably, the alkoxide species (Scheme 1) is a deprotonated form of either A or C. Knözinger also derived kinetic equations from this mechanistic model but found that these did not fit the experimental data for the reaction of ethanol on alumina. This led Knözinger to conclude that kinetic analysis is not a helpful tool for elucidating the actual mechanism of the ether formation (23).

Also, based on a comparative study of the dehydration reaction of methanol on alumina and silica–alumina, Figueras *et al.* (26) postulated an alternate mechanism for ether formation. In this mechanism the methanol is dissociatively adsorbed on acid–base pairs to form  $\text{CH}_3^+$  and  $\text{OH}^-$  species in parallel with the production of  $\text{CH}_3\text{O}^-$  and  $\text{H}^+$  species.

The mechanism of alkene formation is much more fully understood. The elegant work of Knözinger *et al.* (6, 25, 27) showed that alkene formation on alumina occurs



SCHEME 1. Mechanistic model for the formation of ether from alcohols (21, 23, 24).

through an  $E_2$ -like reaction mechanism in which the alcohol is first adsorbed on the alumina surface by the interaction with a surface hydroxyl and oxide pair (D). The reaction then proceeds through the transition state (E), during which a molecule of water is released as the double bond forms. Knözinger and co-workers (25, 27) and Yamaguchi and Tanabe (9) showed that oxide ions and hydroxyl groups are essential for alkene production but that Lewis acid sites are apparently not involved.

Therefore, despite the many spectroscopic and reactor studies, there is still no detailed understanding of the mechanism of ether formation. We have developed a technique to study the temperature-programmed desorption (TPD) of alcohols adsorbed on oxides using the probe of the mass spectrometer as the reactor. We have studied the products of a series of aliphatic alcohols and have extended the research to the use of [ $^{18}\text{O}$ ]methanol and [ $^{18}\text{O}$ ]ethanol. The [ $^{18}\text{O}$ ] ethanol study, to our knowledge, is the first of its kind. The TPD results of [ $^{18}\text{O}$ ]methanol and [ $^{18}\text{O}$ ]ethanol adsorbed on  $\gamma$ -alumina show that there are two routes to alkoxide formation; this is contrary to the findings of the earlier work. The results described in this paper shed a great deal of light on the mechanism of ether formation from the dehydration of alcohols on  $\gamma$ -alumina.

#### EXPERIMENTAL

Norton 6375C (20/40 mesh)  $\gamma$ -alumina was used in this study. The surface area is  $221.8 \text{ m}^2/\text{g}$  and the pore volume  $1.4 \text{ cm}^3/\text{g}$ . The  $\gamma$ -alumina was calcined in flowing air ( $60 \text{ cm}^3/\text{min}$ ) at  $500^\circ\text{C}$  for 3 h. The calcined alumina was stored in an air-tight container. Care was taken to ensure that the alumina was exposed to the air for as little time as possible.

#### FT-IR Procedure

IR spectra were collected using a Nicolet 170 SX FT-IR spectrometer with a liquid nitrogen-cooled MCT detector. All spectra were recorded after 100 scans with a resolu-

tion of  $4 \text{ cm}^{-1}$ . Spectra were measured using a quartz cell with NaCl windows attached to a glass gas handling/vacuum system. A self-supporting wafer, 1.6 cm in diameter, was prepared by first grinding the sample to 325 mesh size and then pressing 20 mg of the powder at 6000 psi. The wafers were then mounted in the cell and dried by heating the sample to  $300^\circ\text{C}$  for 2 h while under evacuation. The dried sample was then exposed to 45 Torr ethanol (absolute ethanol) for 5 min followed by evacuation. The temperature of the evacuated sample was then raised and the FT-IR spectra were recorded at various temperatures. This experiment was repeated using  $\text{CH}_3\text{CH}_2\text{OD}$ .

#### TPD Procedure

The mass spectrometer used was a Finnigan-MAT TSQ70 instrument. The mass spectrometer was scanned from 12 to 170 Da every 0.5 s and the source was operated at  $150^\circ\text{C}$  using a 70-eV ionizing potential with an ion current of  $200 \mu\text{A}$  under electron impact conditions.

Adsorption of the alcohols was achieved by vapor deposition: about 0.2 g of alumina was exposed to the vapor of approximately 0.5 ml of the alcohol for 1 h in an air-tight container. About 0.2 mg of each alumina-alcohol sample was placed into a glass insertion tube, which was loaded into the temperature-programmed probe of the mass spectrometer and immediately inserted into the source chamber of the mass spectrometer with minimal exposure to air. The pressure of the source of the mass spectrometer was  $1 \times 10^{-7}$  Torr. The temperature of the sample was increased from 25 to  $300^\circ\text{C}$  at a rate of  $25^\circ\text{C}$  per min. The probe is within 1 mm of the ionizing electrons, which ensures that the desorbed species are analyzed immediately upon desorption from the alumina surface. This situation minimizes diffusion losses and time delays and is therefore much more sensitive than typical temperature-programmed experiments.

For the poisoning experiment, about 0.2 g of alumina was exposed to the vapors of

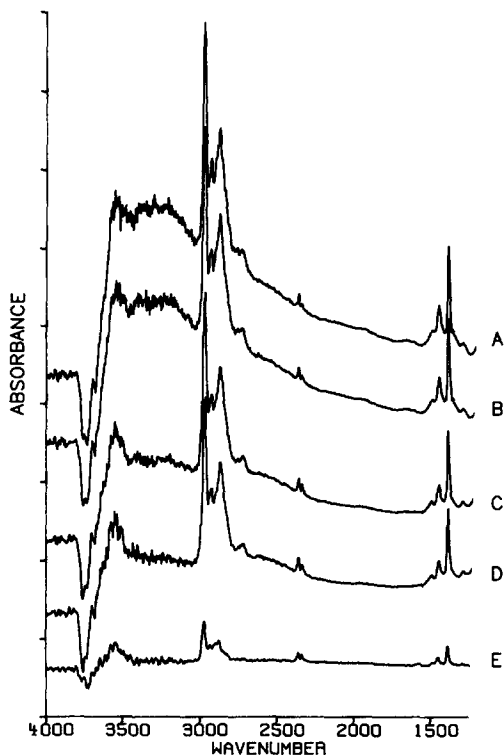


FIG. 1. IR spectra of  $\text{CH}_3\text{CH}_2\text{OH}$  adsorbed on  $\gamma$ -alumina followed by evacuation at: (A) room temperature; (B)  $50^\circ\text{C}$ ; (C)  $100^\circ\text{C}$ ; (D)  $150^\circ\text{C}$ ; and (E)  $300^\circ\text{C}$  and cooling to room temperature.

0.25 ml of 2,6-dimethylpyridine for 24 h. The alumina was then transferred to a clean vessel and exposed to the vapors of 0.5 ml of [ $^{18}\text{O}$ ]ethanol.

#### RESULTS AND DISCUSSION

##### *IR Analysis of the Reactions of $\text{CH}_3\text{CH}_2\text{OH}$ and $\text{CH}_3\text{CH}_2\text{OD}$ on Calcined $\gamma$ -Alumina*

Figure 1A contains the IR spectrum produced when  $\text{CH}_3\text{CH}_2\text{OH}$  (45 Torr) is adsorbed onto dried  $\gamma\text{-Al}_2\text{O}_3$  and the sample is then evacuated for 5 min at  $1 \times 10^{-5}$  Torr. IR bands are observed at 2874, 2930, and  $2972\text{ cm}^{-1}$ , which can be assigned to the C–H stretching vibrations of the ethyl group; also evident are bands at 1384 and  $1447\text{ cm}^{-1}$ , which are due to C–H and C–H<sub>2</sub> deformations of the ethyl group. A broad

signal centered at  $3420\text{ cm}^{-1}$ , which is attributed to the OH stretching band of physisorbed ethanol, is observed. There is also a broad signal centered at  $3560\text{ cm}^{-1}$ , and negative bands at 3621, 3721, and  $3760\text{ cm}^{-1}$ . This spectrum is very similar to that obtained by Knözinger and co-workers (15, 16) and is due to the presence of physisorbed ethanol in addition to both types of chemisorbed species, A and C. According to Knözinger and Stübner (16), the negative signals in the hydroxyl region are due to the formation of species C. Upon evacuation at temperatures of up to  $150^\circ\text{C}$  (Figs. 1B–1D), there is a small decrease in the intensities of the bands around 2900 and  $1450\text{ cm}^{-1}$ , and the signal around  $3420\text{ cm}^{-1}$  has disappeared. The disappearance of the  $3420\text{ cm}^{-1}$  band shows that all the physisorbed ethanol has been removed from the alumina surface. Evacuation at  $300^\circ\text{C}$  and subsequent cooling to room temperature (Fig. 1E) results in a large decrease in the intensities of all the signals compared to the signals in the spectrum obtained prior to the heat treatment (Fig. 1A). This decrease is due to a depletion of alkoxide species on the alumina surface; however, this experiment provides no information concerning the desorption process and products.

A similar experiment was performed using  $\text{CH}_3\text{CH}_2\text{OD}$  (Fig. 2). Adsorption of  $\text{CH}_3\text{CH}_2\text{OD}$  followed by a 15-min evacuation at room temperature produces signals at 1384 and  $1447\text{ cm}^{-1}$  (due to C–H deformations of the ethyl group) and at 2874, 2930, and  $2972\text{ cm}^{-1}$  (due to C–H stretching vibrations of the ethyl group). Negative signals are observed at 3606, 3658, 3680, 3727, and  $3760\text{ cm}^{-1}$ , and there is a broad, intense feature between 2000 and  $2600\text{ cm}^{-1}$ . Some of the negative signals (3606, 3727, and  $3760\text{ cm}^{-1}$ ) are due to the presence of species C; however, some of these signals can be attributed to OD formation via hydrogen/deuterium exchange. Evidence for the formation of OD bonds is provided by the appearance of bands around  $2600\text{ cm}^{-1}$ . Evacuation at temperatures up to  $150^\circ\text{C}$  (Figs. 2B–2D) results in the

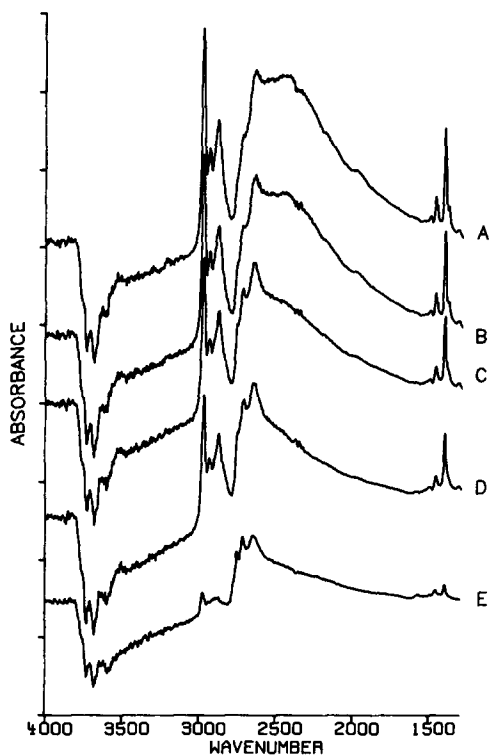


FIG. 2. IR spectra of  $\text{CH}_3\text{CH}_2\text{OD}$  adsorbed on  $\gamma$ -alumina followed by evacuation at (A) room temperature; (B)  $50^\circ\text{C}$ ; (C)  $100^\circ\text{C}$ ; (D)  $150^\circ\text{C}$ ; and (E)  $300^\circ\text{C}$  and cooling to room temperature.

disappearance of the band at  $2400\text{ cm}^{-1}$ ; the  $2400\text{ cm}^{-1}$  band is therefore due to physisorbed  $\text{CH}_3\text{CH}_2\text{OD}$ , which is desorbed at the higher temperatures. A signal at  $3560\text{ cm}^{-1}$  remains and can be attributed to species C. As with the  $\text{CH}_3\text{CH}_2\text{OH}$ , evacuation to  $300^\circ\text{C}$  results in the desorption of many of the alkoxide species.

These IR experiments show that alkoxide species, as well as physisorbed ethanol, are present on the alumina surface after exposure to ethanol. Evacuation at elevated temperatures causes the desorption of physisorbed ethanol and, at higher temperatures, the loss of alkoxide species. However, this experiment yields information on the adsorption process only; no information concerning the desorption reactions and products can be obtained.

### TPD Analysis of the Reactions of Aliphatic Alcohols on $\gamma$ -Alumina

Reconstructed partial ion chromatograms of the reaction of 1-propanol on calcined alumina are shown in Fig. 3. Initially, at  $25^\circ\text{C}$ , only desorption of physisorbed water and alcohol is observed as evidenced by the selected traces of  $m/z = 17, 18$  and  $m/z = 59, 60$ . As the temperature increases, two products are observed: the lower temperature product on the  $m/z = 73, 102$  trace can be assigned as dipropyl ether, and the higher temperature product is the propene, which gives a signal at  $m/z = 41, 42$ . These products are the result of dehydration reactions. Evidence for the coproduction of water is seen in the  $m/z = 17, 18$  ion trace, which shows two broad peaks corresponding to the formation of the ether and the alkene. The ether : alkene ratio is calculated to be 1 : 32. Table 1 summarizes the important peak temperatures and areas of the signals. No signals due to the desorption of the alcohol are observed at temperatures above  $100^\circ\text{C}$ , which confirms the conclusion from our IR work that no physisorbed alcohol remains on the alumina surface. Also, no other signals due to hydrocarbons or carboxylate decomposition products were detected, presumably since such species are only produced at temperatures above  $300^\circ\text{C}$  (10, 30).

We have repeated the TPD experiments on a series of alcohols in order to investigate the effect of alcohol structure on the production of alkene and ether. The reconstructed partial ion chromatograms of the reaction of methanol are shown in Fig. 4. Methanol yields only dimethyl ether, as evidenced by the signal at  $m/z = 46$ . Again, no other hydrocarbon signals were observed in the total mass spectrum. However, at the high-temperature end of the  $m/z = 46$  signal there is a shoulder. The presence of this shoulder indicates that dimethyl ether is formed in another reaction, which is only operative at higher temperatures (onset  $250^\circ\text{C}$  in Fig. 4). We suggest that this process involves the reaction of a methoxy group bound at a less reactive or less accessible surface site.

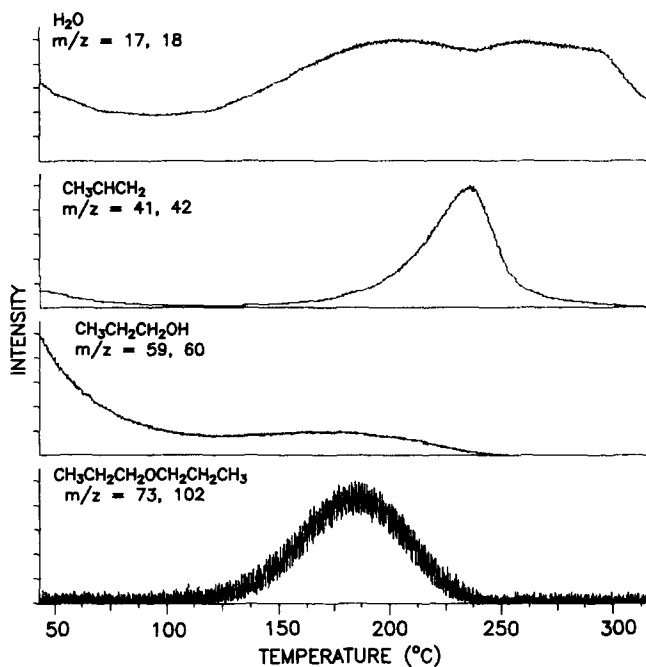


FIG. 3. Reconstructed partial chromatograms of the temperature-programmed desorption products of 1-propanol adsorbed on  $\gamma$ -alumina.

TABLE I

Summary of Peak Temperatures and Areas for the Products from TPD of Alcohols Adsorbed on  $\gamma$ -Alumina

Alcohol	Product	Peak temp. (°C)	Peak areas	Ratio ROR : C=C
CH <sub>3</sub> OH	ROR	194 (256) <sup>a</sup>		
	C=C	—		
CD <sub>3</sub> CD <sub>2</sub> OH	ROR	213	$9.20 \times 10^6$	
	C=C	288	$2.90 \times 10^8$	1 : 33
CH <sub>3</sub> CH <sub>2</sub> CH <sub>2</sub> OH	ROR	185	$2.97 \times 10^6$	
	C=C	226	$9.70 \times 10^7$	1 : 32
(CH <sub>3</sub> ) <sub>2</sub> CHOH	ROR	163	$4.99 \times 10^5$	
	C=C	175	$9.97 \times 10^8$	1 : 2000
CH <sub>3</sub> CH <sub>2</sub> C(CH <sub>3</sub> ) <sub>2</sub> OH	ROR	—	0.00	
	C=C	124	$2.64 \times 10^8$	
CH <sub>3</sub> <sup>18</sup> OH	R <sup>16</sup> OR	243	$1.71 \times 10^8$	
	R <sup>18</sup> OR	193	$2.52 \times 10^8$	
CH <sub>3</sub> CH <sub>2</sub> <sup>18</sup> OH	R <sup>16</sup> OR	220	$4.95 \times 10^6$	
	R <sup>18</sup> OR	179	$1.59 \times 10^7$	
	C=C	261	$3.42 \times 10^8$	
2,6-Dimethylpyridine	R <sup>16</sup> OR	275	$1.37 \times 10^6$	
	R <sup>18</sup> OR	220	$8.51 \times 10^5$	
CH <sub>3</sub> CH <sub>2</sub> <sup>18</sup> OH	C=C	289	$3.10 \times 10^7$	

<sup>a</sup> Approximate temperature of the shoulder.

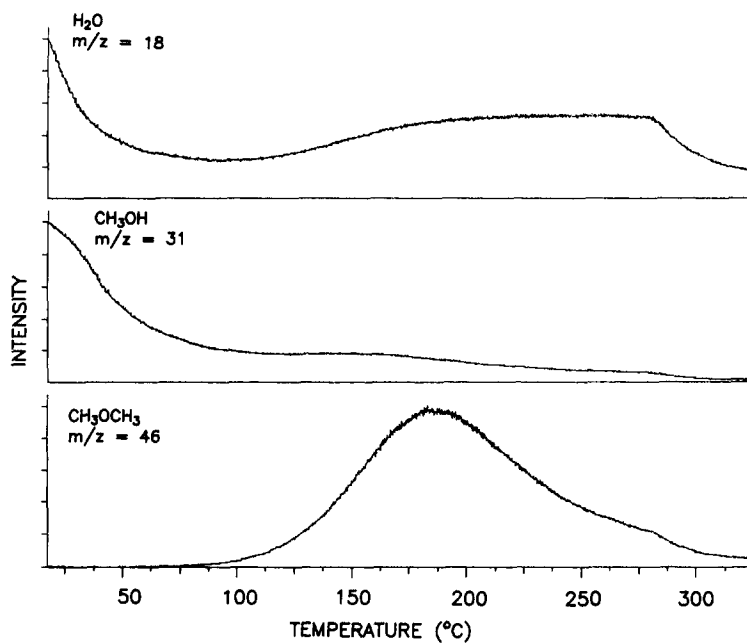


FIG. 4. Reconstructed partial chromatograms of the temperature-programmed desorption products of methanol adsorbed on  $\gamma$ -alumina.

Figure 5 shows the reconstructed partial chromatograms of the products of the reactions of  $\text{CD}_3\text{CD}_2\text{OH}$  with the alumina surface. Again, the lower-temperature product is the ether ( $m/z = 84$ ), and the higher-temperature product is the alkene. The ether:alkene ratio is 1:33. It should be noted that these ratios are calculated on the basis of products formed over the duration of the entire run. Clearly, the production of ether is highly favored during the early stages of the reaction. Also shown in Fig. 5 are the ion traces for  $\text{H}_2\text{O}$  ( $m/z = 18$ ) and DHO ( $m/z = 19$ ). There is a continual loss of  $\text{H}_2\text{O}$  from the alumina surface as the temperature is raised, as evidenced by the continuous, broad signal on the  $m/z = 18$  trace. This is probably due to the dehydroxylation of the alumina surface (6). DHO is the elimination product from  $\text{CD}_3\text{CD}_2\text{OH}$  and it is observed that the  $m/z = 19$  signal has a maximum that corresponds to the signal maximum of the  $m/z = 32$  ( $\text{CD}_2\text{-CD}_2$ ) species. We also observed a very weak signal on the ion trace

for  $m/z = 20$ , which is due to  $\text{D}_2\text{O}$  (the ratio of DHO to  $\text{D}_2\text{O}$  is 12:1). This indicates that there is some scrambling of the alkyl hydrogens with either the alumina surface or the hydrogen of the alcohol hydroxyl.

The results of the reactions of isopropanol are shown in Fig. 6, and the peak temperatures and areas are summarized in Table 1. While both the alkene ( $m/z = 42$ ) and ether ( $m/z = 73, 102$ ) are produced, the ratio of ether to alkene is now 1:2000. Also, it can be seen that the temperature at which the alkene is produced is  $156^\circ\text{C}$  (compared to  $226^\circ\text{C}$  for 1-propanol), showing that the isopropoxide is less stable toward  $\text{E}_2$  elimination than the 1-propoxide. The reaction of tertiary amyl alcohol ( $\text{C}_2\text{H}_5\text{C}(\text{CH}_3)_2\text{OH}$ ) produces alkene as the only product, with no ether formation observed (Table 1).

The observation that primary alkoxides exhibit ether formation prior to alkene formation indicates that the former is the kinetically favored process in this system. This is true even though ether formation is a bi-

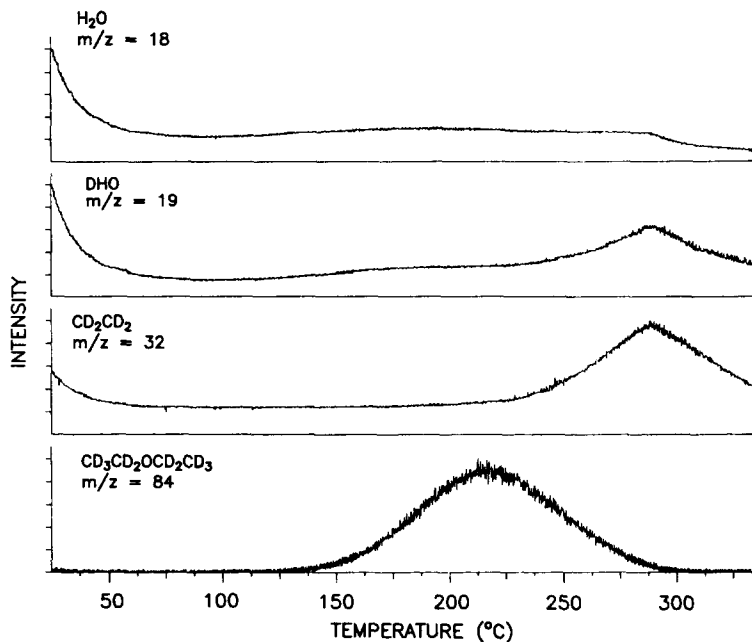


FIG. 5. Reconstructed partial chromatograms of the temperature-programmed desorption products of  $\text{CD}_3\text{CD}_2\text{OH}$  adsorbed on  $\gamma$ -alumina.

molecular reaction requiring the participation of alkoxides on adjacent sites (23, 24), with alkene presumably resulting from the unimolecular elimination of water from a single alkoxide (25, 27). It is tempting to attribute this behavior to a proximity effect, such that the ether formation (favored at high surface alkoxide coverage) results in partial depletion of the alkoxides; the remaining alkoxides are isolated and thus forced to undergo the unimolecular reaction resulting in alkene. This suggestion is based in part on the observation of a shoulder on the high-temperature end of the chromatogram peak for dimethyl ether ( $m/z = 46$ , Fig. 4); the methoxide species responsible for the less facile ether-forming process may correspond to the species that would give alkene in the reactions of higher alkoxide homologues. While we believe that the proximity effect is partially responsible for the observed desorption chemistry, our labeling studies (discussed below) indicate that there are also fundamental differences in the nature of the alkoxide sites giving rise to the observed products.

From the data in Table 1, it can be seen that the size and structure of the alkoxide both determine the relative ratio of elimination products and the temperature at which the reactions occur. The primary alkoxides (ethoxy and propoxy) give similar ether:alkene product ratios, and this ratio decreases as branching (and thus number of  $\beta$ -hydrogens) increases; similar results have been obtained in the reactions of alcohols with  $\text{MgO}$  and  $\text{TiO}_2$  (28–30). Finally, we note again that there is no evidence in any of the systems for the production of any surface carbonates (**B**) or products derived therefrom; this is consistent with the claim that these oxidation products result only at high adsorption temperatures (31).

#### *TPD Analysis of [ $^{18}\text{O}$ ]Ethanol and [ $^{18}\text{O}$ ]Methanol Reactions on $\gamma$ -Alumina*

In order to learn more about the nature of the alkoxide species giving rise to the observed products, we have carried out TPD experiments using [ $^{18}\text{O}$ ]ethanol and [ $^{18}\text{O}$ ]methanol. The partial ion chromato-



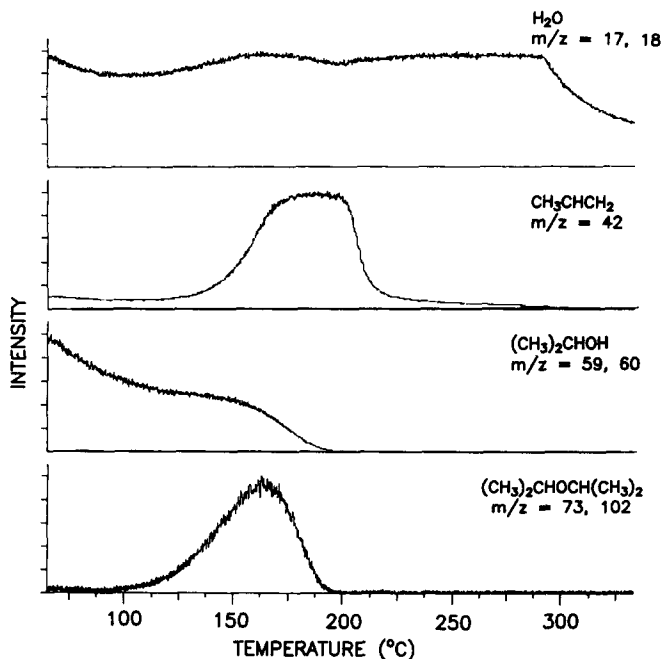


Fig. 6. Reconstructed partial chromatograms of the temperature-programmed desorption products of isopropanol adsorbed on  $\gamma$ -alumina.

grams for the reaction of [ $^{18}\text{O}$ ]methanol on  $\gamma\text{-Al}_2\text{O}_3$  are shown in Fig. 7. The reaction produces two isotopomeric ether products as evidenced by the ion chromatograms for  $m/z = 45, 46$  and  $m/z = 47, 48$ . These correspond to molecular ions that are derived from  $\text{CH}_3^{16}\text{OCH}_3$  and  $\text{CH}_3^{18}\text{OCH}_3$ , respectively. The  $^{18}\text{O}$ -containing ether is produced at lower temperatures than the  $^{16}\text{O}$ -containing ether. Also, it can be seen that the signal due to the  $\text{CH}_3^{16}\text{OCH}_3$  exhibits a shoulder at the higher temperature. As expected, both  $\text{H}_2^{16}\text{O}$  ( $m/z = 18$ ) and  $\text{H}_2^{18}\text{O}$  ( $m/z = 20$ ) are produced during the reaction.

The results of the reaction of [ $^{18}\text{O}$ ]ethanol are shown in Fig. 8. Again, in addition to the two water isotopomers and the ethene ( $m/z = 26, 28$ ), this reaction produces two isotopomeric ether products as evidenced by the signals on the ion chromatograms for  $m/z = 59, 74$  and  $m/z = 61, 76$ ; these correspond to  $\text{CH}_3\text{CH}_2^{16}\text{OCH}_2\text{CH}_3$  and  $\text{CH}_3\text{CH}_2^{18}\text{OCH}_2\text{CH}_3$ , respectively. As with

[ $^{18}\text{O}$ ]methanol, the ether incorporating the  $^{18}\text{O}$  is the first product to appear. A summary of the peak temperatures and peak areas appears in Table 1. If a portion of the  $\text{Al}_2\text{O}_3$ -[ $^{18}\text{O}$ ]ethanol sample is studied via TPD and then the remaining sample is allowed to stand in a closed container for 1 week (room temperature), additional TPD studies indicate that the [ $^{16}\text{O}$ ]ether:[ $^{18}\text{O}$ ]ether ratio, the ether:alkene ratio, and the observed desorption temperatures remain virtually unchanged. Thus, there is no evidence of alkoxide scrambling on the surface, suggesting that the alkoxides are formed irreversibly.

The two isotopomeric ether products originate from two different alkoxide species, one incorporating an  $^{18}\text{O}$ , the other  $^{16}\text{O}$ . The presence of these two alkoxides suggests that alkoxide is formed via two routes, one involving a direct reaction at a Lewis site (resulting in deprotonation of the complexed alcohol and formation of  $^{18}\text{O}$ -labeled alkoxide, Scheme 2 top) and the other in-

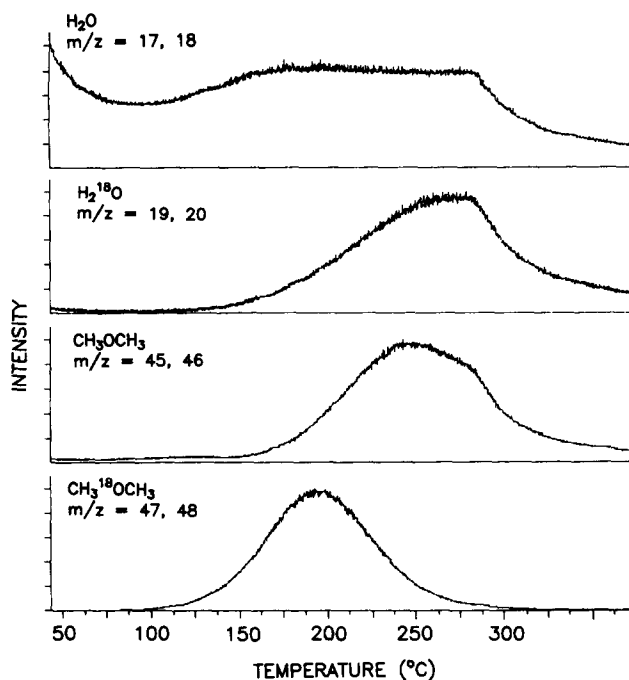


FIG. 7. Reconstructed partial chromatograms of the temperature-programmed desorption products of  $[^{18}\text{O}]$ methanol adsorbed on  $\gamma$ -alumina.

volving a reaction with a nucleophilic surface base site (resulting in  $^{18}\text{OH}$  displacement and the formation of  $^{16}\text{O}$ -labeled alkoxide, Scheme 2 bottom). This latter pathway probably involves a secondary interaction of the alcohol hydroxyl with an adjacent acid site, since hydroxide itself is a relatively poor leaving group.

Further evidence that the ethers are formed from different alkoxide species was obtained by carrying out a poisoning experiment using 2,6-dimethylpyridine. 2,6-Dimethylpyridine is a base that is expected to adsorb onto either Brønsted acid sites or Lewis acid sites (32). Adsorption of 2,6-dimethylpyridine prior to  $[^{18}\text{O}]$ ethanol adsorption is seen to have a significant effect on the ratio of  $[^{16}\text{O}]$ ether to  $[^{18}\text{O}]$ ether (Fig. 9). This ratio for the alumina/ $[^{18}\text{O}]$ ethanol sample is 1:3 while it is 1:0.6 when the alumina had been exposed to the 2,6-dimethylpyridine prior to ethanol adsorption (Table 1). This clearly demon-

strates that the ether isotopomers are formed from different alkoxide species and that the  $[^{18}\text{O}]$ ether is formed from an alkoxide associated with Lewis acid sites. These studies also argue against the formation of an  $^{16}\text{O}$ -labeled alkoxide at a Brønsted acid site (via protonolysis of alcohol hydroxide), since the latter would be strongly inhibited by the pretreatment with 2,6-dimethylpyridine; this would have led to a decrease in the  $[^{16}\text{O}]$ ether: $[^{18}\text{O}]$ ether ratio, rather than the observed increase. The aging studies described above also indicate that the nucleophilic and acidic sites retain their characteristic differences long after alkoxide formation.

Additionally, the 2,6 dimethylpyridine-poisoned surface generates the ethers and alkene at higher temperatures than the surface without the poison (Table 1). It also changes the alkene to ether ratios. These differences can be attributed to the presence of the 2,6-dimethylpyridine on the alumina

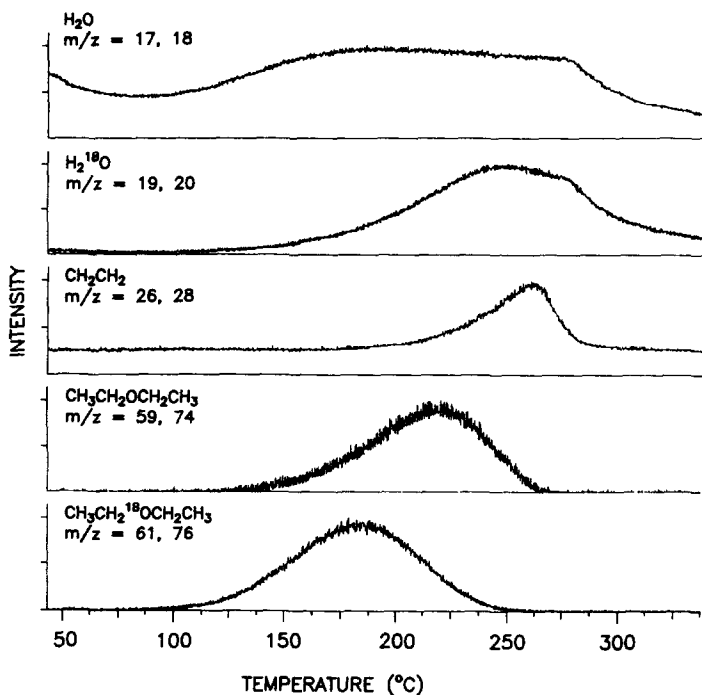
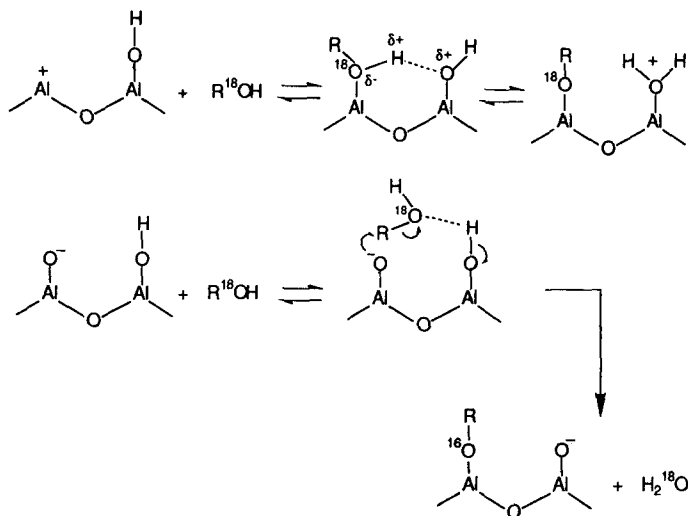


FIG. 8. Reconstructed partial chromatograms of the temperature-programmed desorption products of [ $^{18}\text{O}$ ]ethanol adsorbed on  $\gamma$ -alumina.

surface, which lowers the surface coverage of the alkoxides and promotes the unimolecular reaction.

The TPD and IR data presented here show

that alkenes are formed from alkoxides and not adsorbed molecular alcohols, as suggested by Knözinger *et al.* (25); the alkoxide is formed on basic sites as concluded by



SCHEME 2. Two routes to alkoxide formation on the alumina surface.

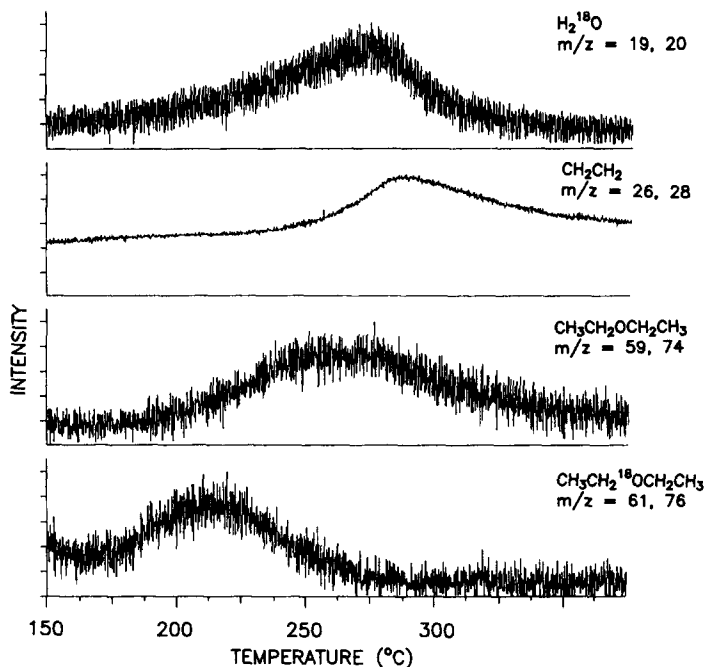


FIG. 9. Reconstructed partial chromatograms of the temperature-programmed desorption products of ethanol- $^{18}\text{O}$  adsorbed on  $\gamma$ -alumina after exposure of the alumina to 2,6-dimethylpyridine.

some researchers (33). Indeed, recent studies of MgO showed that relatively high selectivities for alkenes were obtained via base-catalyzed dehydration of alcohols (29). Also, these data show that the alkene and some ether are formed on the same surface sites, which is contrary to the early conclusions that ether and alkenes are formed on different sites (21).

Identification of two isotopomeric ethers show that there are two routes to alkoxide formation. This suggests that the mechanism postulated by Knözinger *et al.* (23) and Padmanabhan and Eastburn (24) for ether formation is not the only mechanistic route. Also, our IR and TPD data show that there is no physisorbed alcohol present on the catalyst surface at the temperature at which ether formation takes place; the reaction is therefore between two alkoxide species and not an alkoxide and a molecularly adsorbed alcohol. The mechanism suggested by Figueras *et al.* (26) for the reaction of methanol

on alumina is consistent with the appearance of the [ $^{16}\text{O}$ ]ether.

#### CONCLUSION

TPD studies of adsorbed alcohols using the probe of the mass spectrometer as the reactor yield results similar to those obtained by TPD using flow-reactor systems (10) or high-vacuum systems (28–33). Our studies of various alcohols suggest that the facility with which various alkoxides undergo the two elimination processes is dependent on the size of the alkyl groups and the degree of branching.

From our analysis of  $^{18}\text{O}$ -labeled alcohols adsorbed on dried (but partially hydroxylated) calcined  $\gamma$ -alumina we can make several conclusions concerning the alcohol adsorbing sites and the possible mechanisms of the dehydration reactions:

1. Our data show conclusively that at the temperatures at which ether formation occurs no physisorbed alcohol is present on

the alumina surface. This indicates that ether formation cannot involve a reaction between alkoxide and physisorbed alcohol, in contrast to the suggestions of Jain and Pillai (21) and Knözinger *et al.* (23).

2. Surface-bound alkoxides are formed by two routes: (a) dissociative adsorption on Lewis acid sites and (b) nucleophilic attack by a surface oxide on an alcohol that is probably activated toward C–O cleavage. The operation of two pathways and the involvement of two different surface sites are conclusively demonstrated for the first time by use of labeled alcohols and the mass spectrometry technique described herein.

3. Studies involving pretreatment with 2,6-dimethylpyridine confirm that the ether isotopomers are formed from different alkoxide species. In addition, time studies indicate that there is no scrambling of  $^{16}\text{O}$  and  $^{18}\text{O}$  alkoxides between the different types of surface sites after a week at room temperature.

4. With proper standardization and quantitation, the methods described herein should be useful in determining the relative numbers of active acid and base sites on the alumina surface.

In conclusion, we have demonstrated the use of a novel isotopic labeling/mass spectrometric technique for the investigation of the reactions of alcohols on  $\gamma$ -alumina. The sensitivity of the measurement, which is a consequence of the close proximity of the source of the mass spectrometer to the desorbing surface, is an important aspect of the technique. This work shows that this method will be extremely useful in probing the acid–base chemistry of catalyst supports, and ongoing efforts are directed toward similar studies of other oxide supports.

#### REFERENCES

1. Tanabe, K., "Solid Acids and Bases." Academic Press, New York, 1970.
2. Kung, M. C., and Kung, H. H., *Catal. Rev.-Sci. Eng.* **27**, 425 (1985).
3. Tanabe, K., in "Catalysis by Acids and Bases" (B. Imelik, C. Naccache, G. Coudurier, Y. Ben Taarit, and J. C. Vedrine, Eds.), Vol. 20, p. 1. Elsevier, Amsterdam, 1985.
4. Benesi, H. A., and Windquist, B. H. C., in "Advances in Catalysis" (D. D. Eley, H. Pines, and P. B. Weisz, Eds.), Vol. 27, p. 98. Academic Press, New York, 1978.
5. Tanabe, K., Misono, M., Ono, Y., and Hattori, H., "New Solid Acids and Bases," Vol. 51. Elsevier, Amsterdam, 1989.
6. Knözinger, H., and Ratnasamy, P., *Catal. Rev.-Sci. Eng.* **17**, 3731 (1978).
7. John, C. S., and Scurrill, M. S., Eds., in "Catalysis," Vol. 1, p. 136. The Chemical Society, 1977.
8. Davis, B. H., in "Adsorption and Catalysis on Oxide Surfaces" (M. Che and G. C. Bond, Eds.), p. 309. Elsevier, Amsterdam, 1985.
9. Yamaguchi, T., and Tanabe, K., *Bull. Chem. Soc. Jpn.* **47**, 424 (1974).
10. Matsushima, T., and White, J. M., *J. Catal.* **44**, 183 (1976).
11. Bandiera, J., and Naccache, C., *Appl. Catal.* **69**, 139 (1991).
12. Little, L. H., "Infrared Spectra of Adsorbed Species." Academic Press, New York, 1966.
13. Hair, M. L., "Infrared Spectroscopy in Surface Chemistry." Dekker, New York, 1967.
14. Greenler, R. G., *J. Chem. Phys.* **37**, 2091 (1962).
15. Jeziorowski, H., Knözinger, H., Meye, W., and Müller, H. D., *J. Chem. Soc. Faraday Trans. 1* **69**, 1744 (1973).
16. Knözinger, H., and Stübner, B., *J. Phys. Chem.* **82**, 1526 (1978).
17. Lavalley, J. C., Caillod, J., and Travert, J., *J. Phys. Chem.* **84**, 2084 (1980).
18. Hattori, T., Shirai, K., Niwa, N., and Murakami, Y., *React. Kinet. Catal. Lett.* **15**, 193 (1980).
19. Benaissa, M., Saur, O., and Lavalley, J. C., *Mater. Chem.* **7**, 699 (1982).
20. Maatman, R. W., and Vande Griend, L. J., *J. Catal.* **20**, 238 (1971).
21. Jain, J. R., and Pillai, C. N., *J. Catal.* **9**, 322 (1967).
22. de Mourgues, L., Peyron, F., Trambouze, Y., and Prettre, M., *J. Catal.* **7**, 117 (1967).
23. Knözinger, H., Kochloeff, K., and Meye, W., *J. Catal.* **28**, 69 (1973).
24. Padmanabhan, V. R., and Eastburn, F. J., *J. Catal.* **24**, 88 (1972).
25. Knözinger, H., Bühl, H., and Kochloeff, K., *J. Catal.* **24**, 57 (1972).
26. Figueras, F., Nohl, A., de Mourgues, L., and Trambouze, Y., *Trans. Faraday Soc.* **67**, 1155 (1971).
27. Knözinger, H., and Scheglila, A., *J. Catal.* **17**, 252 (1970).
28. Kim, K. S., and Barteau, M. A., *J. Mol. Catal.* **63**, 103 (1990).
29. Peng, X. D., and Barteau, M. A., *Langmuir* **7**, 1426 (1991).

30. Kim, K. S., and Barteau, M. A., *Surf. Sci.* **223**, 13 (1989).
31. Hertl, W., and Cuenca, A. M., *J. Phys. Chem.* **77**, 1120 (1973).
32. Matulewicz, E. R. A., Kerhof, F. P. J. M., Moulign, J. A., and Reitsma, H. J., *J. Colloid Interface Sci.* **77**, 110 (1980).
33. Bowker, M., Houghton, H., and Waugh, K. C., *J. Chem. Soc. Faraday Trans. 1* **78**, 2573 (1982).